

†Research supported by the U. S. Atomic Energy Commission.

¹P. M. Endt and C. Van der Leun, Nucl. Phys. A105, 1 (1967).

²J. W. Olness, W. Haerberli, and H. W. Lewis, Phys. Rev. 112, 1702 (1958).

³C. E. Moss, Nucl. Phys. A145, 423 (1970).

⁴R. A. Morrison, Nucl. Phys. A140, 97 (1970).

⁵D. H. Youngblood, R. L. Kozub, R. A. Kenefick, and J. C. Hiebert, Phys. Rev. C 2, 477 (1970).

⁶R. L. Kozub and D. H. Youngblood, Phys. Rev. C 4, 535 (1971).

⁷Received from P. D. Kunz, University of Colorado.

⁸R. H. Bassel, Phys. Rev. 149, 791 (1966).

⁹J. C. Hiebert, E. Newman, and R. H. Bassel, Phys.

Rev. 154, 898 (1967).

¹⁰C. M. Perey and F. G. Perey, Phys. Rev. 152, 923 (1966).

¹¹B. H. Wildenthal, J. B. McGrory, E. C. Halbert, and H. D. Graber, to be published.

¹²B. Castel, K. W. C. Stewart, and M. Harvey, Nucl. Phys. A162, 273 (1971).

¹³F. W. Prosser, Jr., J. W. Gordan, and L. A. Alexander, Bull. Am. Phys. Soc. 15, 566 (1970).

¹⁴M. C. Mermaz, C. A. Whitten, Jr., and D. A. Bromley, Bull. Am. Phys. Soc. 13, 675 (1968). See also Ref. 11.

¹⁵J. P. Schiffer, Nucl. Phys. 46, 246 (1963).

¹⁶Received from F. G. Perey, ORNL.

¹⁷Y. Hirao, J. Phys. Soc. Japan 16, 1828 (1961).

¹⁸See, e.g., R. L. Kozub, Phys. Rev. 172, 1078 (1968).

PHYSICAL REVIEW C

VOLUME 5, NUMBER 2

FEBRUARY 1972

Reactions Induced by He³ Ions on Zn⁶⁴ †

D. F. Crisler,* H. B. Eldridge,‡ and R. Kunselman

Department of Physics, University of Wyoming, Laramie, Wyoming 82070

and

C. S. Zaidins

Department of Physics, University of Colorado, Boulder, Colorado 80300

(Received 6 August 1971)

Foils of enriched Zn⁶⁴ (99.85%) were bombarded with He³ particles with energies of 22.2, 29.5, 37.7, and 43.4 MeV after which γ -ray spectra were accumulated from the radioactive foils with a large Ge(Li) detector and a 4096-channel pulse-height analyzer system. The isotopes produced were determined by the β -delayed γ rays and their corresponding half-lives. No chemical separation of the foils was performed.

Cross sections for a particular reaction were determined for each isotope and beam energy. The resulting excitation functions for the 13 reactions which were detected are presented, and are compared with similar reactions including those induced by He³ on Cu isotopes. Possible reaction mechanisms are discussed. Direct reactions appear to be the principal reaction mechanism, especially at higher He³-particle energies where cluster-transfer reactions are common.

INTRODUCTION

The origin of this research was a cooperative effort between the Nuclear Physics Laboratory of the University of Wyoming and the Cyclotron Laboratory of the University of Colorado to produce the unreported isotope Ge⁶⁴. It was envisioned that this isotope could be produced by bombarding a highly enriched target of Zn⁶⁴ with He³ particles to produce the compound nucleus Ge^{67*}. If the compound nucleus were produced with sufficient excitation energy, then the emission of three neutrons to yield Ge⁶⁴ should become one possible reaction.

The first attempts to produce Ge⁶⁴ revealed vast gaps in the knowledge of the reactions which are induced by He³ on Zn⁶⁴. Very little was known about the type of reaction, direct or compound-nu-

clear, which might take place, the kinds of particles likely to be emitted, or the cross sections for these reactions. Thus before a systematic search for Ge⁶⁴ could be done, these properties needed to be defined. The type and cross sections for the reactions induced and an indication of the type of reaction induced were found to be somewhat distinguishable by subsequent detection of the radioisotopes produced.

The use of He³ nuclei as accelerated particles for the study of nuclear reactions has increased steadily,¹⁻⁸ since a practical means of obtaining He³ has been developed. Owing to the small binding energy of He³ it is possible to produce compound nuclei with sufficient excitation energy to cause multiple-particle evaporation at relatively low bombarding energies. This makes He³ particles

superior to α particles for certain types of experiments. However, as seen in this experiment, and in similar experiments for He^3 on copper isotopes,^{4,9} He^3 particles are much more likely to induce direct reactions. This results in the process of three-neutron emission becoming much less favorable than that for reactions which form compound nuclei.

A considerable amount of work has been reported on the reaction mechanism which takes place when α particles are used as projectiles on isotopes of masses 55–68^{9–13} and some on zinc isotopes.^{12,13} The reaction-mechanism studies for incident He^3 particles have as yet not been as complete,^{2,3,14} and nearly all the results of interest to this project have been done on copper isotopes.^{4,15–17} Very little has been done with He^3 on Zn^{64} . Only differential cross sections have been reported for the $(\text{He}^3, \alpha)^{18,19}$ and $(\text{He}^3, d)^{19}$ reactions, both at 18-MeV He^3 energies.

Recoil-range^{4,9} and angular-distribution^{15,16} measurements of the recoils in copper targets with statistical theory analysis^{14,20} of the recoil range and excitation functions reveal that α -particle-induced reactions proceed almost entirely by compound-nucleus formation and decay, whereas He^3 -induced reactions are more likely to proceed by direct reactions, often of the stripping or pickup type. Saha and Porile^{4,9} suggest that at higher energies both α - and He^3 -induced reactions may proceed by a direct reaction followed by emission of a second particle by the excited nucleus.

This paper is mainly concerned with the reporting of the experimentally determined excitation functions for 13 reactions which were induced by He^3 particles incident upon a separated Zn^{64} target. All of these reactions were studied by measuring the half-life and the characteristic γ rays emitted by the radioactive isotopes produced. The results obtained are compared with similar reactions resulting from He^3 on copper isotopes. Since Cu^{63} has the same number of neutrons as Zn^{64} and only one less proton, similar reactions and excitation functions might be expected from incident He^3 particles. A discussion of the excitation-function curves, the probable reaction mechanisms, and an analysis of experimental errors follow.

EXPERIMENTAL APPARATUS AND PROCEDURES

The material for the targets consisted of highly enriched (99.85%) Zn^{64} foil²¹ of about 14-mg/cm² thickness. The targets were cut to about 1 cm² in area. Only one piece of target foil was bombarded in each run. The major contaminant in the target material was Zn^{66} of the order of 0.14%. All other

contaminants were less than spectrographic detection limits which were generally 0.02%.

The mounted target and target holder were placed in the bombardment facility of the 52-in. fixed-field alternating-gradient cyclotron²² at the University of Colorado facilities at Boulder, Colorado. The cyclotron is equipped with a He^3 recirculation system which makes He^3 operation economical.

Immediately after bombardment each radioactive target was transported by aircraft to the University of Wyoming at Laramie as quickly as possible. Unlike most other experiments of this type no radiochemical separation of the isotopes was performed, but instead the target was used as a radioactive source as it was. No source of error was introduced by chemical-separation procedures. The average time from end of bombardment to beginning of radioactive counting was about 1 $\frac{1}{4}$ h.

The target (source) was placed at reproducible distances from the front face of the detector. The incoming γ rays were detected by a 22.6-cm³ Ge(Li) coaxial crystal. These pulses from the crystal were fed into a preamplifier, from there to a linear amplifier, and finally into a 4096-channel pulse-height analyzer (PHA). Once a suitable spectrum was accumulated, the contents of the memory of the PHA were recorded on magnetic tape for further analysis using a computer.

EXPERIMENTAL DATA, CALCULATIONS, AND RESULTS

The interaction of an incoming He^3 particle and a Zn^{64} nucleus often results in a final nucleus which can undergo β decay. It makes no difference whether the reaction took place by compound-nucleus formation or a direct reaction, the resulting nuclei undergo β decay which takes them nearer the line of stability. In our case the resulting nuclei are proton-rich, so they usually undergo β^+ decay or electron capture.

When a nucleus undergoes β decay, the resultant daughter nucleus may be left in an excited state, which then emits a γ ray or rays, finally reaching the ground state. It is these γ -ray energies and half-lives which are used to identify the quantity and type of each isotope present.

Spectra were accumulated from each target (source) for times ranging from about 1 h up to 1 $\frac{1}{2}$ yr after bombardment. The accumulation or counting period varied from 400 sec to about 24 h depending upon the length of time after bombardment. The counting period was kept short immediately after bombardment so as to have several points to determine the half-life for the short-half-life isotopes, and the counting periods were gradu-

TABLE I. Beam current and target properties.

Bombardment code name	Target density (mg/cm ²)	Total integrated beam charge (μA/sec)	He ³ -particle energy (MeV)	He ³ -particle energy corrected (MeV)
NINA	12.6	7500	22.2	21.1
PIMA	14.6	3060	29.5	28.7
ROSE	15.3	2340	37.7	37.0
SUE	14.5	2400	43.43	42.8

ally lengthened as the shorter-half-life isotopes decayed away. In all, about 50 spectra were accumulated for each target bombardment.

Figure 1 is a plot of a spectrum taken as soon as possible after bombardment. Most of the γ lines present are due to the short-half-life isotopes which decay quickly, namely Ge⁶⁵, Zn⁶³, and Cu⁶⁰. This particular spectrum was from the bombardment for 37.7-MeV He³ particles. A spectrum taken some hours after bombardment (4–20 h) reveals the intermediate-half-life isotopes (Cu⁶¹, Zn⁶², Cu⁶⁴, Ga⁶⁶, Ge⁶⁶) with the γ lines of Ga⁶⁶ being especially prominent at higher energies (>1 MeV). In a spectrum taken later (>50 h) after bombardment, the long-half-life isotopes become evident. These are Ni⁵⁷, Co⁵⁷, Co⁵⁸, Zn⁶⁵, and Ga⁶⁷.

The activity of the sample from a particular γ ray was determined from the area under the peak of interest by a computer code. This was done for each γ ray over the total number of spectra in which this γ ray appeared. For each bombardment, this consisted of analyzing about 50 peaks, from as few as five spectra to as many as 35 spectra. Wherever possible γ rays of at least three different energies from each isotope were analyzed so as to give a check on the consistency of the data. Only 50 peaks were completely analyzed in each bombardment, but over 150 peaks in all had to be accounted for.

Bombardments were performed using He³-particle energies of 22.2, 29.5, 37.7, and 43.4 MeV. The beam current striking the target was kept in the neighborhood of 1 μA. Bombardments with higher beam currents had been tried, but damage to the targets resulted. Therefore data for these runs were not used. Table I is a summary of incident beam particle energies, average beam particle energies corrected for energy loss in the target,²³ target densities, and total integrated beam current. The corrected He³-particle energy value used was the incident particle energy minus half the average loss of He³ particles traversing the target.

The isotopes, γ rays, activities of the target, and measured half-lives from these γ rays for each bombardment are given in Table II. The half-life for each isotope as stated in the literature is

given in parentheses below the isotope. Note that the activities (C_{γ}) as given in Table II are not the total activity of the target due to a given isotope. These listed activities have not yet been corrected for detector efficiency or for the number of times per 100 decays of the isotope that it will decay by emitting a γ ray of that particular energy.

The cross section for the production of the isotopes associated with the detected γ rays could now be calculated. Table III is a summary of the γ rays analyzed and the cross sections of the isotopes associated with each γ ray. The average cross section for each isotope for each bombardment is also given.

In addition to the γ rays listed in Table II, several other γ rays were detected which could not be associated with any known isotope. These γ rays and their activities and half-lives as measured by the detector are given in Table IV. These activities are not corrected for detector efficiency or for branching ratios of the nucleus leading to a γ ray of that particular energy. This correction was impossible, since the latter quantity is not known. Therefore, the cross sections associated with these unknown γ rays could not be calculated.

The computation and inclusion of errors had to be done in three different phases of the data analysis. First, for each bombardment, the determination of the half-life of an isotope produced is only dependent upon the statistics of counting of a particular energy γ ray and an indeterminate experimental error. The activity of the target as measured due to a particular γ ray is also dependent upon these sources of error. The uncertainties of the half-lives and γ -ray activities expressed in Tables II and IV include these sources.

Secondly, experimental errors associated with the intensity and detector efficiency for each γ ray must be included. The values of the cross sections given for each γ ray in Table III take these sources into account.

Finally, the quoted value for the average cross section (Table III) for the formation of any given isotope is found by the method of weighted averages. The total error for each cross section measured includes the uncertainties in the integrated beam current.

TABLE II. Experimentally determined intensities and half-lives of γ rays from isotopes produced in each bombardment.

Isotope (half-life)	γ ray (keV)	21.3 MeV			28.7 MeV			37.0 MeV			42.8 MeV		
		C_{γ_0} (counts/sec)	$T_{1/2}$ (h)	C_{γ_0} (counts/sec)	$T_{1/2}$ (h)	C_{γ_0} (counts/sec)	$T_{1/2}$ (h)	C_{γ_0} (counts/sec)	$T_{1/2}$ (h)	C_{γ_0} (counts/sec)	$T_{1/2}$ (h)		
Ni ⁵⁷ (35.94 h)	1378	0.0326 ± 0.0067	37.9 ± 7.6	0.289 ± 0.011	34.3 ± 0.9		
Co ⁵⁷ (270 day)	122	0.164 ± 0.005	300 ± 63	1.109 ± 0.007	287 ± 11		
	136	0.141 ± 0.005	244 ± 53		
Co ⁵⁸ (71.3 day)	811	0.433 ± 0.003	70.8 ± 0.9	0.520 ± 0.004	70.4 ± 1.0		
	1322	113 ± 26	26.4 ± 2.2	753 ± 56	24.4 ± 0.6		
Cu ⁶⁰ (24.0 min)	1792	34 ± 19	28.0 ± 6.2	255 ± 32	25.3 ± 1.1		
	284	195 ± 5	3.37 ± 0.05	1727 ± 7	3.33 ± 0.01	1120 ± 10	3.27 ± 0.01	987 ± 6	3.35 ± 0.01	...	3.35 ± 0.01		
Cu ⁶¹ (3.41 h)	373	112.6 ± 1.6	3.39 ± 0.02	110.8 ± 1.6	3.38 ± 0.02		
	656	46.1 ± 1.8	3.50 ± 0.09	428.8 ± 2.0	3.35 ± 0.01	250.8 ± 1.7	3.39 ± 0.01	250.6 ± 1.6	3.35 ± 0.01	...	3.35 ± 0.01		
Zn ⁶² (9.3 h)	1185	9.56 ± 1.17	3.50 ± 0.25	78.2 ± 0.7	3.30 ± 0.02	46.4 ± 0.5	3.33 ± 0.01	44.5 ± 0.6	3.36 ± 0.02	...	3.36 ± 0.02		
	260	42.9 ± 1.0	9.24 ± 0.08	3.13 ± 0.24	10.1 ± 0.4		
Zn ⁶³ (38.4 min)	394	40.7 ± 1.0	9.35 ± 0.14	3.11 ± 0.20	10.1 ± 0.4		
	548	169.2 ± 0.9	9.25 ± 0.02	91.1 ± 0.5	9.18 ± 0.03	14.74 ± 13	9.34 ± 0.05	16.64 ± 0.16	9.35 ± 0.06	...	9.35 ± 0.06		
Cu ⁶⁴ (12.82 h)	597	252.4 ± 1.2	9.21 ± 0.02	129.6 ± 1.0	9.31 ± 0.04	21.5 ± 0.18	9.41 ± 0.04	27.7 ± 0.2	9.33 ± 0.06	...	9.33 ± 0.06		
	670	263 ± 34	41.4 ± 2.3	305 ± 33	40.0 ± 1.9	646 ± 9	38.8 ± 0.5	1487 ± 26	38.4 ± 0.2	...	38.4 ± 0.2		
Zn ⁶⁵ (243.8 day)	962	138 ± 34	44.3 ± 5.3	158 ± 17	40.2 ± 1.7	323 ± 13	39.3 ± 0.7	735 ± 17	38.7 ± 0.3	...	38.7 ± 0.3		
	1346	0.396 ± 0.088	13.8 ± 1.4	0.268 ± 0.021	13.6 ± 0.7	0.348 ± 0.029	12.4 ± 1.7	...	12.4 ± 1.7		
Ga ⁶⁵ (15.2 min)	1115	7.18 ± 0.09	258 ± 4	3.37 ± 0.04	246 ± 5	0.675 ± 0.003	251 ± 6	0.657 ± 0.004	252 ± 6	...	252 ± 6		
	61	(9.8 ± 1.4)10 ⁴	14.6 ± 0.4	(5.5 ± 1.3)10 ⁴	14.1 ± 0.7	(6.6 ± 2.6)10 ³	16.4 ± 1.6	(3.8 ± 2.7)10 ³	18.4 ± 3.7	...	18.4 ± 3.7		
Ga ⁶⁶ (9.5 h)	115	(4.32 ± 0.28)10 ⁵	15.0 ± 0.2	(2.16 ± 0.98)10 ⁵	15.2 ± 0.14	(4.3 ± 0.3)10 ⁴	15.8 ± 0.3	(3.88 ± 0.40)10 ⁴	15.6 ± 0.4	...	15.6 ± 0.4		
	153	(5.8 ± 1.1)10 ⁴	15.1 ± 0.5	(3.27 ± 0.87)10 ⁴	15.1 ± 0.87	(4.7 ± 2.3)10 ³	16.9 ± 2.2		
Zn ⁶⁸ (12.82 h)	207	(6.0 ± 3.5)10 ³	18.1 ± 3.8		
	752	730 ± 430	16.4 ± 2.4	475 ± 350	17.1 ± 6.8	...	17.1 ± 6.8		
Ga ⁶⁸ (9.5 h)	833	28.8 ± 0.5	9.43 ± 0.07	15.4 ± 0.25	9.39 ± 0.07	3.40 ± 0.11	9.36 ± 0.17	3.02 ± 0.10	9.87 ± 0.22	...	9.87 ± 0.22		
	1039	129.2 ± 0.8	9.47 ± 0.02	69.30 ± 0.67	9.59 ± 0.05	15.6 ± 0.14	9.55 ± 0.04	14.6 ± 0.2	9.60 ± 0.06	...	9.60 ± 0.06		
Ni ⁶⁹ (12.82 h)	1919	1.74 ± 0.11	9.41 ± 0.23	0.406 ± 0.034	9.30 ± 0.42		
	2190	7.80 ± 0.19	9.46 ± 0.09		
2752	24.7 ± 0.24	9.44 ± 0.04	12.58 ± 0.15	9.54 ± 0.05	2.85 ± 0.077	9.59 ± 0.08	2.80 ± 0.051	9.49 ± 0.11	...	9.49 ± 0.11			

TABLE II (Continued)

Isotope (half-life)	γ ray (keV)	21.3 MeV		28.7 MeV		37.0 MeV		42.8 MeV	
		C_{γ_0} (counts/sec)	$T_{1/2}$ (h)	C_{γ_0} (counts/sec)	$T_{1/2}$ (h)	C_{γ_0} (counts/sec)	$T_{1/2}$ (h)	C_{γ_0} (counts/sec)	$T_{1/2}$ (h)
Ge ⁶⁶ (2.23 h)	109	407 ± 12	2.41 ± 0.05	234 ± 10	2.43 ± 0.06	66.5 ± 9.5	2.33 ± 0.20	51.6 ± 4.6	2.50 ± 0.10
	182	156 ± 23	2.42 ± 0.22	70.2 ± 13.4	2.47 ± 0.28
	190	127 ± 13	2.25 ± 0.17	67.3 ± 13.6	2.58 ± 0.33
	382	253 ± 11	2.23 ± 0.07	138 ± 6	2.28 ± 0.06	53.8 ± 8.6	1.69 ± 0.15	30.4 ± 2.9	2.23 ± 0.10
	471	55.0 ± 5.1	2.22 ± 0.13	12.3 ± 2.2	2.49 ± 0.21
Ga ⁶⁷ (78 h)	537	39.8 ± 3.1	2.44 ± 0.12	25.4 ± 2.6	2.04 ± 0.14
	706	28.1 ± 1.6	2.26 ± 0.10	9.1 ± 2.8	2.39 ± 0.44
	93	15.8 ± 0.17	78.5 ± 1.5	7.87 ± 0.07	78.2 ± 1.2	1.76 ± 0.03	84.7 ± 2.3	2.25 ± 0.04	79.1 ± 1.4
	185	5.83 ± 0.17	69.7 ± 3.6	2.73 ± 0.03	84.2 ± 1.1	0.728 ± 0.020	90.7 ± 4.2	0.890 ± 0.039	83.8 ± 4.4

The determination of the half-life and the initial activity of the target due to a γ ray of particular energy was done by the method of a least-squares fit to the \log_{10} of the activities vs time. The uncertainty in the half-life and the initial activity (C_{γ_0}) from a γ ray of given energy were found by the method outlined by Jaffey.²⁴ The count rate, uncertainty in the count rate, and the effect of background count rate for each γ ray were used for this computation. In a few cases, the uncertainties in the half-lives as determined from several γ rays of different energies from the same isotope were not sufficient to give agreement on half-life values. To compensate for this an indeterminate experimental error was introduced, using criteria given by Beers²⁵ and the χ^2 test as defined by Jaffey.²⁴ In almost all cases a 1% indeterminate error was used; in no case was more than a 2.5% error needed. Some of the sources of this indeterminate error could be the uncertainties in the positions of the target (source) and the value of the time after bombardment.

In the second phase of error analysis, the main sources of error which were accounted for were the quoted uncertainties in the absolute intensities of the emitted γ rays and the absolute efficiency of the detector. The latter was taken to be 5% for all γ -ray energies. These sources of error were combined with the statistical errors outlined above by the rules for combining independent errors.^{25,26} The results are shown in Table III in the columns labeled cross sections.

Finally, the uncertainty in the total integrated beam current was included. This was done after the cross section for formation for each isotope had been calculated by the method of weighted averages²⁵ from the cross sections determined by each γ ray associated with a given isotope. The integrated beam current was assumed to be known to within $\pm 10\%$. This uncertainty was included as an independent error. The final error values for the cross sections measured are given in Table III in the columns labeled Ave.

INTERPRETATION AND DISCUSSION OF EXPERIMENTAL RESULTS

For the ease and convenience of plotting the data and for helpfulness in the discussion of experimental results, the reactions will be treated as He³ + Zn⁶⁴ forming a Ge⁶⁷ nucleus with subsequent emission or evaporation of particles by the highly excited nucleus. However, it is emphasized here that several of the reactions are much more likely to proceed directly, often by a stripping or pickup reaction, and that a composite nucleus is not formed in these cases. The reactions are also presented

TABLE III. Calculated cross sections from experimental data for reactions induced by He³ on Zn⁶⁴.

Isotope	γ ray (keV)	21.3 MeV		28.7 MeV		37.0 MeV		42.8 MeV	
		Cross section (mb)	Ave. (mb)	Cross section (mb)	Ave. (mb)	Cross section (mb)	Ave. (mb)	Cross section (mb)	Ave. (mb)
Ni ⁵⁷	1378	0.0455 ± 0.009	0.0455 ± 0.0099	0.413 ± 0.027	0.413 ± 0.049
	122	3.36 ± 0.20	3.36 ± 0.39	12.8 ± 0.66	13.2 ± 1.4
	136	14.8 ± 1.29	...
Co ⁵⁸	811	11.1 ± 0.56	11.1 ± 1.2	13.6 ± 0.69	13.6 ± 1.5
	1322	2.34 ± 0.76	2.26 ± 0.67	15.6 ± 1.51	15.5 ± 2.0
Cu ⁶⁰	1792	2.07 ± 1.15	...	15.3 ± 2.16	...
	284	9.46 ± 0.74	...	86.8 ± 6.5	...	136.4 ± 10.3	...	124.9 ± 9.3	...
Cu ⁶¹	373	108.4 ± 10.2	...	110.8 ± 10.4	...
	656	7.56 ± 0.45	8.11 ± 0.89	72.7 ± 4.7	75.1 ± 8.1	103.2 ± 6.7	108.8 ± 11.6	107.2 ± 6.9	109.4 ± 11.6
Zn ⁶²	1185	8.46 ± 1.18	...	71.6 ± 4.6	...	103.0 ± 6.7	...	102.7 ± 6.7	...
	260	39.4 ± 2.2	7.43 ± 0.69
Zn ⁶³	394	38.8 ± 2.3	7.65 ± 0.63
	548	37.0 ± 1.9	38.4 ± 4.0	20.9 ± 1.1	20.9 ± 2.2	8.33 ± 0.44	8.15 ± 0.86	9.66 ± 0.51	9.86 ± 1.06
	597	38.9 ± 2.1	...	21.0 ± 1.2	...	8.56 ± 0.47	...	10.11 ± 0.56	...
Cu ⁶⁴	670	11.0 ± 1.7	10.5 ± 1.8	12.3 ± 1.7	12.9 ± 1.8	56.4 ± 4.6	57.8 ± 6.9	142.8 ± 11.7	146 ± 17
	962	12.4 ± 3.3	...	13.7 ± 2.1	10.4 ± 2.8	61.0 ± 7.0	17.3 ± 2.5	152.6 ± 16.8	23.1 ± 3.4
Zn ⁶⁵	1346	10.4 ± 2.6
Ga ⁶⁵	1115	718 ± 38	718 ± 81	355 ± 19	355 ± 40	177 ± 9.1	177 ± 20	177 ± 9.1	177 ± 20
	61	390 ± 78	...	197 ± 86	...	44.7 ± 19.8	...	30.0 ± 22	...
Ga ⁶⁶	115	344 ± 31	351 ± 45	155 ± 71	182 ± 46	58.2 ± 5.4	57.3 ± 7.7	61.3 ± 7.3	58.0 ± 9.0
	153	385 ± 112	...	197 ± 67	...	53.3 ± 28.4
Ge ⁶⁶	207	253 ± 186
	752	69.1 ± 42.2	...	52.4 ± 39.5	...
Ge ⁶⁶	833	26.8 ± 2.6	...	14.9 ± 1.4	...	14.9 ± 1.4	...	7.44 ± 0.74	...
	1039	27.4 ± 2.0	28.6 ± 3.1	15.3 ± 1.1	15.2 ± 1.66	8.51 ± 0.63	8.47 ± 0.93	8.20 ± 0.61	8.15 ± 0.91
Ge ⁶⁶	1919	14.9 ± 1.8	...	8.61 ± 1.16
	2190	31.0 ± 2.5
Ge ⁶⁶	2752	29.6 ± 2.4	...	15.5 ± 1.3	...	8.63 ± 0.72	...	8.79 ± 0.74	...
	109	3.93 ± 0.52	...	2.31 ± 0.31	...	1.57 ± 0.30	...	1.27 ± 0.20	...
Ge ⁶⁶	182	4.30 ± 0.84	...	1.98 ± 0.47
	190	3.60 ± 0.64	...	1.95 ± 0.49
Ga ⁶⁷	382	4.53 ± 0.32	4.34 ± 0.49	2.53 ± 0.18	2.51 ± 0.28	2.36 ± 0.40	1.85 ± 0.30	1.39 ± 0.15	1.39 ± 0.18
	471	3.21 ± 0.47
Ga ⁶⁷	537	4.60 ± 0.59	...	3.00 ± 0.43	1.79 ± 0.38	...
	706	8.05 ± 2.1	...	2.67 ± 1.06
Ga ⁶⁷	93	1087 ± 216	1186 ± 176	576 ± 114	604 ± 89	318 ± 63	370 ± 55	421 ± 84	477 ± 72
	185	1242 ± 163	...	619 ± 80	...	408 ± 54	...	516 ± 70	...

in the usual manner, that is, it is assumed that the particles given off are neutrons, protons, or α particles. The data will be discussed in terms of mass-one, -two, -three, and higher-mass emissions. However, one reaction is likely to be due to the impurity Zn⁶⁶ in the target.

In general the data will be compared with similar He³ reactions on Cu⁶³ and Cu⁶⁵ wherever possible. Literature on He³ reactions on Cu isotopes is more abundant and has been acquired more recently than α -induced reactions on Zn⁶⁴, but it seems more realistic to compare results with other He³ experiments, since the type of reaction caused by He³ as opposed to α particles is quite different.^{4,9}

One-Particle-Emission Reactions

The three reactions of interest here are Zn⁶⁴-(He³, n)Ge⁶⁶, Zn⁶⁴(He³, p)Ga⁶⁶, and Zn⁶⁴(He³, α)Zn⁶³. The excitation functions for these reactions are plotted in Fig. 2. Also plotted in the same figure are curves from other works which are similar in nature and which partially cover the same energy range of He³ particles.

The long, high-energy tails of the (He³, n) and (He³, p) curves of Fig. 2 for Zn⁶⁴ suggest the mechanism for these reactions must be at least partially a direct two-particle-transfer reaction. The work by Saha and Porile⁴ with recoil ranges of the final nucleus for He³ on copper nuclei indeed supports the direct-reaction mechanism hypothesis. Further work by Fujiwara and Porile¹⁶ on the angular distributions of the reaction products for the (He³, n) reaction on Cu⁶⁵, and distorted-wave Born-approximation calculations confirm the two-particle-transfer reaction.

The curves of Fig. 2 show that the He³ particle is far more likely, by about a factor of 10, to transfer a neutron and a proton to the Zn⁶⁴ nucleus than it is to transfer two protons. This result is supported by Golchert, Sedlet, and Gardner (GSG)⁸ for the (He³, n) on Cu⁶⁵ reaction, and by Bryant, Cochran, and Knight (BCK)¹ for the (He³, p) on Cu⁶³ reaction. The comparable excitation functions for Cu and Zn bombarded by He³ particles with two-particle transfers are almost identical in both shape and magnitude. It was necessary to use two

different Cu isotopes here for comparison, since the (He³, p) reaction on Cu⁶⁵ yields the stable isotope Zn⁶⁷.

The Zn⁶⁴(He³, α)Zn⁶³ curve in Fig. 2 is more difficult to interpret. Both GSG⁸ and BCK¹ obtained curves for (He³, α) on Cu⁶³ which are somewhat similar in shape to the (He³, α) on Zn⁶⁴ curve, but they attribute the increase in cross section with increasing He³-particle energy to the reaction Cu⁶⁵-(He³, $\alpha 2n$)Cu⁶², since their targets were not highly enriched in Cu⁶³. However, since the targets used in this study were 99.85% Zn⁶⁴ and only about 0.14% Zn⁶⁶, the possibility of the reaction Zn⁶⁶(He³, $\alpha 2n$)-Zn⁶³ becoming a factor is very remote; this would require a cross section of the order of tens of barns. Saha and Porile⁴ measured the Cu⁶⁵(He³, α)-Cu⁶⁴ excitation function, the shape of which is similar over the same energy range to the Zn⁶⁴(He³, α)-Zn⁶³ curve of Fig. 2. Their sample was highly enriched in Cu⁶⁵ so that the possibility of another reaction mechanism contributing was also remote. If an argument is applied to (He³, α) on Zn⁶⁴ similar to that advanced by Saha and Porile⁴ for (He³, α) on Cu⁶⁵, the curve of Fig. 2 may be explained as follows: The lower-energy portion (20–30 MeV) is due to the reaction Zn⁶⁴(He³, α)Zn⁶³ and the higher-energy part (30–45 MeV) is characterized by either a (He³, He³ n) or (He³, $2p2n$) type reaction. The Q values for these reactions are 9.0, -11.6, and -19.3 MeV, respectively. Thus, as higher He³ energies, the latter two reactions could very likely contribute. For α -induced reactions^{12,13} in Zn⁶⁴, the (α , n) cross section is much higher, by about a factor of 20 at 30 MeV, than is the He³-induced reaction. Also, Porile's¹² (α , n) cross section falls off much faster with increasing energy, indicating compound-nucleus formation rather than direct reaction. However, his curve for the (α , p) excitation function is very similar to ours in magnitude and slope, thus suggesting that some of the (α , p) reaction may be partially direct.

Two-Particle-Emission Reactions

The reactions of interest here are: Zn⁶⁴(He³, np)-Ga⁶⁵, Zn⁶⁴(He³, $2p$)Zn⁶⁵, Zn⁶⁴(He³, αn)Zn⁶²; and Zn⁶⁴-

TABLE IV. Experimentally determined intensities and half-lives of γ rays from unidentified isotopes.

γ -ray energy (keV)	21.3 MeV		28.7 MeV		37.0 MeV		42.8 MeV		$T_{1/2}$ weighted average (h)
	C_{γ_0} (counts/sec)	$T_{1/2}$ (h)	C_{γ_0} (counts/sec)	$T_{1/2}$ (h)	C_{γ_0} (counts/sec)	$T_{1/2}$ (h)	C_{γ_0} (counts/sec)	$T_{1/2}$ (h)	
136	33.2 ± 7.5	2.49 ± 0.40	30.0 ± 7.2	2.39 ± 0.24	2.42 ± 0.21
326	11.8 ± 6.0	2.5 ± 1.2	9.5 ± 3.5	3.09 ± 0.52	3.0 ± 0.5
636	1.0 ± 0.7	6.5 ± 4.0	6.5 ± 4.0
685	3.47 ± 0.72	7.52 ± 0.67	2.18 ± 0.32	7.57 ± 0.47	0.27 ± 0.11	9.5 ± 2.0	0.60 ± 0.31	5.7 ± 1.5	7.5 ± 0.4

($\text{He}^3, 2n$) Ge^{65} , $\text{Zn}^{64}(\text{He}^3, \alpha p)\text{Cu}^{62}$, $\text{Zn}^{64}(\text{He}^3, 2\alpha)\text{Ni}^{59}$. The excitation functions of the first three are plotted in Fig. 3. Similar reactions for He^3 on Cu isotopes are also plotted in the same figure in order to be able to compare the results of other workers.

Because of the short half-life (1.5 min) of Ge^{65} , any Ge^{65} activity would have decayed to Ga^{65} by the time counting of the sample was begun, so that the excitation function for the reaction $\text{Zn}^{64}(\text{He}^3, 2n)\text{Ge}^{65}$ was not determined. Thus the curve for Ga^{65} includes both the $2n$ and np contributions.

Other possible two-particle-emission reactions, given below the dashed line, were not observed or detected for the following reasons. The reaction $\text{Zn}^{64}(\text{He}^3, \alpha p)\text{Cu}^{62}$ yields a short-half-life isotope (9.8 min) which usually decays directly to the ground state of stable Ni^{62} without emission of characteristic γ rays. Two- α -particle-emission results in the isotope Ni^{59} which decays to the ground state of stable Co^{59} without emission of any γ rays.

The shapes of the ($\text{He}^3, 2n$) + (He^3, np), ($\text{He}^3, 2p$), and ($\text{He}^3, \alpha n$) excitation-function curves for He^3 on Zn^{64} resemble the ($\text{He}^3, 2p$) and ($\text{He}^3, \alpha n$) measured

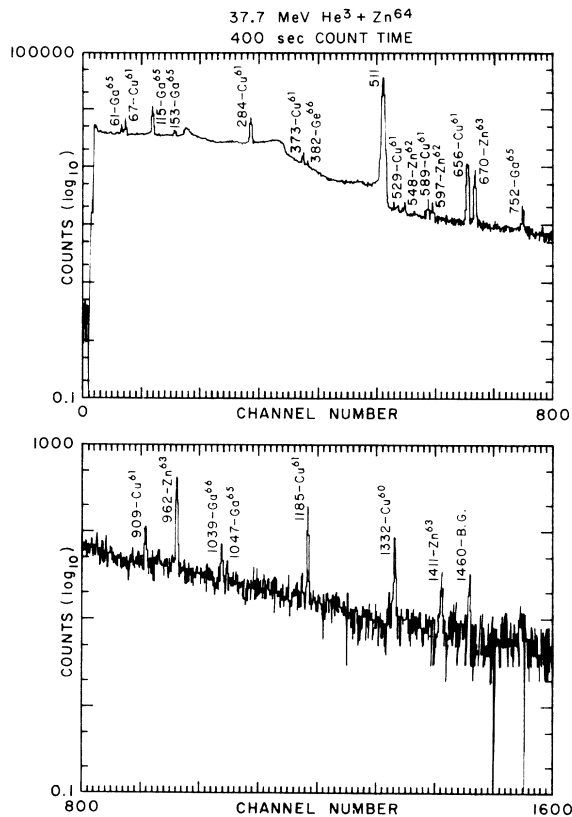


FIG. 1. A γ -ray spectrum taken 1.34 h after end of bombardment of Zn^{64} by 37.7-MeV He^3 particles. The short-half-life isotopes are prevalent.

cross sections¹ for He^3 on Cu^{63} , and also resemble the ($\text{He}^3, 2n$) curves⁸ for He^3 on Cu^{65} , for the energy range of He^3 particles measured in common. However, unlike the one-particle-emission curves above, there is a considerable difference in the magnitude of the measured cross sections for similar reactions using either Zn^{64} or $\text{Cu}^{63,65}$ for target material.

The greatest cross section for this work was found to be the $2p$ -emission reaction, which agrees with the results of King *et al.*²⁷ for He^3 on Si^{28} and of GSG⁸ for He^3 on Cu^{63} . The Zn^{64} cross section is about twice as great as the Cu^{63} value. Conversely, our value for ($\text{He}^3, \alpha n$) on Zn^{64} is about half the value measured for the reaction $\text{Cu}^{63}(\text{He}^3, \alpha n)\text{Cu}^{61}$.⁸ It is more difficult to compare the $2n$ -emission reaction, since our value is the sum of the $2n + np$ emissions. However, our value for the sum is about 5 times as great as the $2n$ emission from He^3 on Cu^{65} as measured by GSG.⁸

A comparison of the magnitudes of the cross sections of Figs. 2 and 3 reveals that two-particle emission ($2p$, $2n + np$, and αn) is generally favored over one-particle emission. This is quite reasonable from energy considerations, since the excitation energy for the composite Ge^{67} nucleus ranges from 31.9 to 52.5 MeV for the incident He^3 bombardments which were made.

Another comparison between Figs. 2 and 3 re-

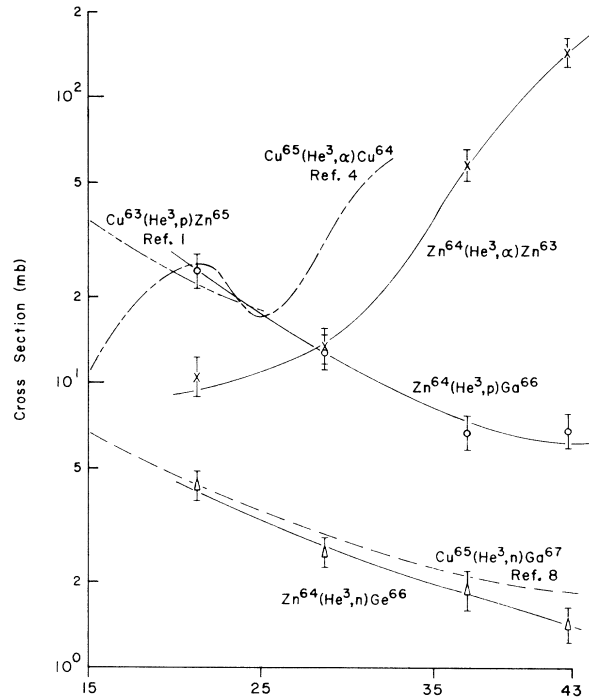


FIG. 2. He^3 on Zn^{64} excitation functions for one-particle emission.

veals that the excitation curves for two-particle emission decrease with energy somewhat more rapidly than do the curves for single-particle emission; compound-nucleus reaction mechanisms are thought to be more prevalent. Direct reactions undoubtedly still contributed, but not as strongly as for single-particle emission.

The mechanism for the reaction $Zn^{64}(He^3, 2p)Zn^{65}$ is likely to be predominantly a single-particle stripping reaction. The significantly larger cross section for the $(He^3, 2p)$ reaction than the $(He^3, np) + (He^3, 2n)$ reactions suggests an additional mechanism must also be operating here. GSG,⁸ who obtained similar results for He³ on Cu⁶³, considered the Oppenheimer-Phillips process as one possibility. In this process, the He³ particle is assumed to be oriented by the Coulomb repulsion such that the neutron of the He³ particle is nearer the Zn⁶⁴ nucleus. Thus the neutron may be attracted by nuclear forces while the two protons remain outside the range of the nuclear forces. This mechanism is a possibility because of the small binding energy of He³.

From the measurement of the recoil range of Ga⁶⁶ for the reaction $Cu^{65}(He^3, 2n)Ga^{66}$, Saha and Porile⁴ deduced that this reaction took place mainly by compound-nucleus formation. The excitation curve, Fig. 3, for the $(He^3, 2n) + (He^3, np)$ reactions on Zn⁶⁴ does not decrease quite as rapidly with increasing He³-particle energy as the curve¹ used by Saha and Porile for reference. This suggests that

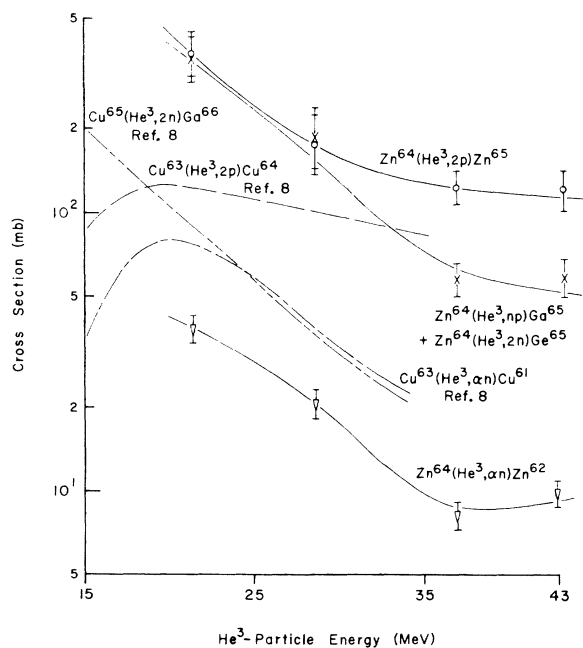


FIG. 3. He³ on Zn⁶⁴ excitation functions for two-particle emission.

the (He^3, np) contribution to the curve may be partially due to direct reactions. The stripping of a proton from the He³ particle is a likely reaction mechanism.

The $(He^3, \alpha n)$ reaction excitation function is shown in Fig. 3, which is compared with a similar type of reaction for He³ on Cu⁶⁵ done by GSG.⁸ Except for a difference in magnitude, the curves agree very well over comparable He³ energies. However, the curve for He³ on Zn⁶⁴ reveals an increase in the cross section for the $(He^3, \alpha n)$ reaction for He³ energies above 37 MeV. A possible explanation is that the $(He^3, He^3 2n)$ reaction channel is opened at higher He³-particle energies. The Q value for this latter reaction is -20.8 MeV.

Excitation function curves^{12,13} for the (α, np) reaction on Zn⁶⁴ are not similar to the $(He^3, np) + (He^3, 2n)$ curve. The α -induced-reaction curves are monotonically increasing up to the limit of measurement (25 MeV) whereas the He³-induced-reaction curve is decreasing over the same energy range. The difference in excitation energy between incidence for He³ and α particles is so large that the reaction mechanisms are probably not the same. In this energy region, compound-nucleus

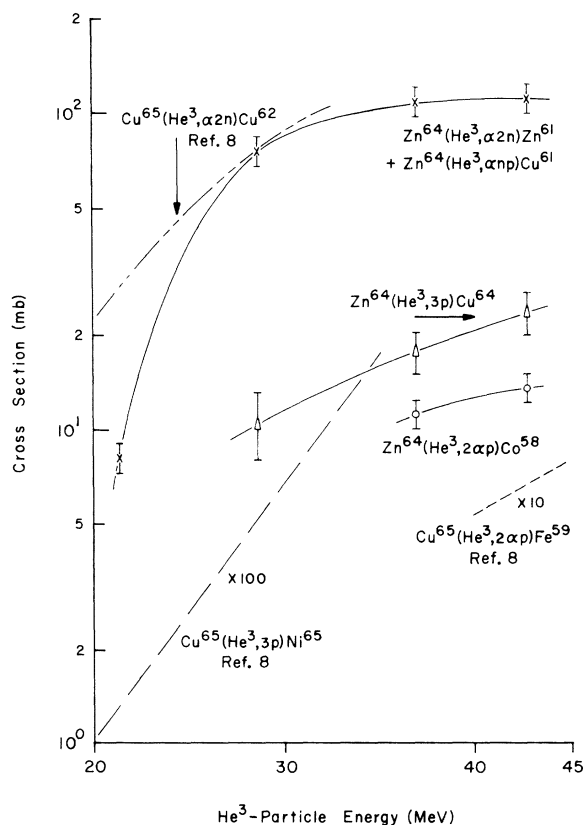


FIG. 4. He³ on Zn⁶⁴ excitation functions for three-particle emission.

formation is dominant for α particles,⁴ while He^3 particles induce direct reactions.⁹

Three-Particle-Emission Reactions

Expressed in terms of n -, p -, and α -particle emission, the reactions below qualify as the three-particle type. As for two-particle emission, the first group of reactions are observed, while those in the second group are not. The reactions are: $\text{Zn}^{64}(\text{He}^3, 3p)\text{Cu}^{64}$, $\text{Zn}^{64}(\text{He}^3, \alpha 2n)\text{Zn}^{61}$, $\text{Zn}^{64}(\text{He}^3, \alpha np)\text{Cu}^{61}$, $\text{Zn}^{64}(\text{He}^3, 2\alpha p)\text{Co}^{58}$; and $\text{Zn}^{64}(\text{He}^3, 3n)\text{Ge}^{64}$, $\text{Zn}^{64}(\text{He}^3, 2np)\text{Ga}^{64}$, $\text{Zn}^{64}(\text{He}^3, 2pn)\text{Zn}^{64}$, $\text{Zn}^{64}(\text{He}^3, \alpha 2p)\text{Ni}^{61}$, $\text{Zn}^{64}(\text{He}^3, 2\alpha n)\text{Ni}^{58}$, $\text{Zn}^{64}(\text{He}^3, 3\alpha)\text{Fe}^{55}$. The excitation functions for the observed reactions are plotted in Fig. 4. Also plotted in the same figure are excitation functions for similar types of reactions induced by He^3 on Cu^{65} .

In general, the magnitudes of these excitation functions are considerably smaller (except for Cu^{61}) than those for one- or two-particle emission. From energy considerations alone, this is to be expected. However, the cross sections for these reactions are increasing very rapidly with increasing He^3 incident energy so that three-particle emission would probably become the dominant reaction

mechanism at slightly higher energies.

The production of Cu^{61} was quite important in all the bombardments as revealed by the large cross section. The amount of Cu^{61} measured was due to the two reactions $\text{Zn}^{64}(\text{He}^3, \alpha 2n)\text{Zn}^{61}$ and $\text{Zn}^{64}(\text{He}^3, \alpha pn)\text{Cu}^{61}$. Because of its short half-life (89 sec), any Zn^{61} formed would have decayed to Cu^{61} by the time counting of the target was begun. Since the Q value for production of Zn^{61} is much more negative than for production of Cu^{61} , as discussed below, it is likely that most of the Cu^{61} measured is produced directly.

If the mechanism for production of the Zn^{61} or Cu^{61} were the evaporation of three particles, $\alpha 2n$ and αnp , respectively, the Q values for these reactions would be -12.8 and -6.6 MeV. Since other reactions with Q values near this do not have cross sections approaching that for the production of Cu^{61} , it appears quite unlikely that Cu^{61} is produced by this mechanism. Instead, the emission of a single particle, He^6 to produce Zn^{61} , or Li^6 to produce Cu^{61} , requires Q values of -11.8 and -2.9 MeV, respectively. Large cross sections for the $(\text{He}^3, \text{Li}^6)$ and $(\text{He}^3, \text{He}^6)$ reactions for He^3 particles on nuclei for isotopic masses up to 30

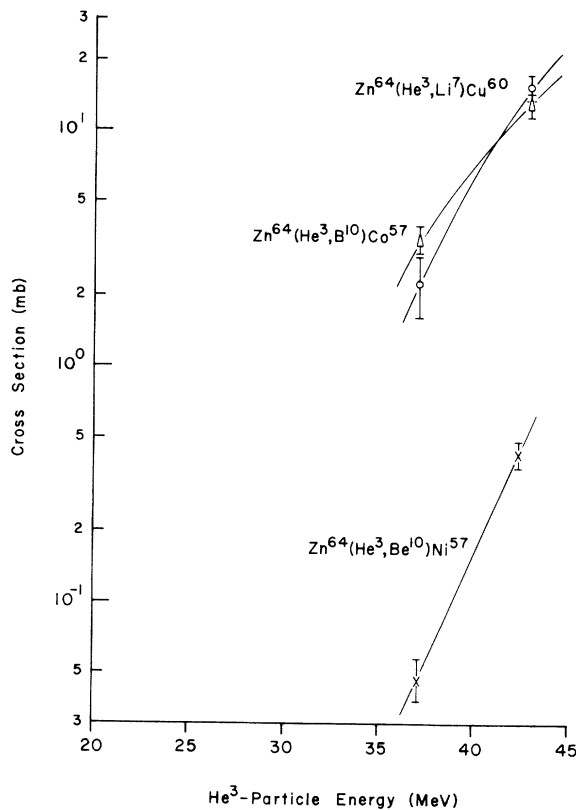


FIG. 5. He^3 on Zn^{64} excitation functions for higher-mass emission.

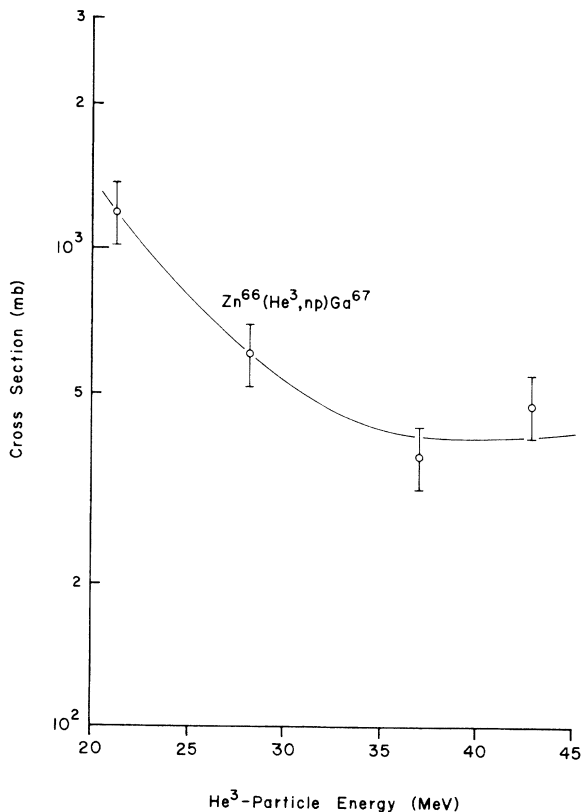


FIG. 6. Excitation function for production of Ga^{67} from He^3 on Zn^{66} impurity in foil.

have been definitely established.²⁸

The excitation function for (He³, α_{2n}) on Cu⁶⁵ from GSG³ is plotted in Fig. 4. The Q value for this reaction is -8.1 MeV which is approximately the same as for the (He³, α_{np}) reaction of Zn⁶⁴. The curves are very similar.

One of the most interesting reactions which resulted is the (He³, 3p) reaction (see Fig. 4). The detection limits for the measurement of the γ ray emitted by Cu⁶⁴ in decaying to Ni⁶⁴ were such that only bombardments with He³ particles above 28.7 MeV produced sufficient quantities of Cu⁶⁴ to be detected. Two possibilities exist for the reaction mechanism involved in 3p emission. The most probable process is a neutron stripping reaction from the He³ particle followed by emission of a proton. By the same reasoning neutron stripping followed by neutron emission should be almost equally as probable. However, the residual nucleus is Zn⁶⁴ again, so that there is no means of detecting this.

The other possibility is compound-nucleus formation with subsequent emission of three protons. If this were the mechanism, then two-proton emission followed by neutron emission, or proton emission followed by two-neutron emission (or tritium emission) should be approximately as probable. This would yield the isotopes Zn⁶⁴ and Ga⁶⁴, respectively. Because of its short half-life, Ga⁶⁴ would not be detected if it were produced, and, of course, Zn⁶⁴ is stable. Three-neutron emission would be yet another three-nucleon-emission possibility, but this reaction has a threshold energy of about 21 MeV. If this reaction did occur, it would yield the isotope Ge⁶⁴, which has not been reported in the literature. In order for us to detect this isotope, its half-life would have to be about 15 min or greater. Also if it were produced, and assuming a half-life greater than 15 min, then the γ rays from Ga⁶⁴ should also be detected. This has not been the case. Further work has been done on the search for Ge⁶⁴, which is discussed in more detail elsewhere.²⁹

The excitation function of Cu⁶⁵ for (He³, 3p) from GSG³ is also plotted in Fig. 4. Over the same energy range the curves for (He³, 3p) are similar in slope but differ in magnitude by nearly a factor of 100.

The (He³, 2α_p) reaction for Zn⁶⁴ is detectable only at He³-particle energies of 37 MeV and above. The excitation function for this reaction as well as for a similar reaction⁸ induced in Cu⁶⁵ is plotted in Fig. 4. Once again, as for the three-proton emission above, the cross section for this reaction in Cu⁶⁵ is much less, by about a factor of 25, than it is for Zn⁶⁴. It is possible the emission mechanism here is a single entity,³⁰ Be⁹, rather than two α particles plus a proton. Thus the reac-

tion would be Zn⁶⁴(He³, Be⁹)Co⁵⁸.

A reaction which should be nearly as probable as the (He³, 2α_p) reaction is Zn⁶⁴(He³, 2α_n)Ni⁵⁸. This cannot be observed, since Ni⁵⁸ is stable. Another three-particle reaction which is not observed is Zn⁶⁴(He³, 3α)Fe⁵⁵. There are no γ rays emitted in the decay of Fe⁵⁵.

Higher-Mass-Emission Reactions

The reactions which will be discussed in this category are Zn⁶⁴(He³, Li⁷)Cu⁶⁰, Zn⁶⁴(He³, Be¹⁰)Ni⁵⁷, and Zn⁶⁴(He³, B¹⁰)Co⁵⁷. These reactions are not expressed in terms of emission of neutrons, protons, and α particles, since it is improbable that they take place in this manner. Instead a single, higher-mass entity is more likely to be emitted. All of the above reactions were observed only for the higher He³ bombardment energies. This is shown by the excitation functions plotted in Fig. 5.

The conclusion that higher-mass emission takes place by emitting a single entity is substantiated in part by GSG³ for higher-mass emissions from He³ on copper isotopes. They were actually able to chemically separate Be⁷ from one of their targets. Other workers^{30,31} have observed direct reactions using He³ particles with emissions of Li⁷ and Be⁷. In our case Be⁷ emission leads to the stable nucleus Ni⁶⁰.

Other Reactions

The detection of γ rays from the isotope Ga⁶⁷ poses an interesting problem. If the Ga⁶⁷ were produced from the Zn⁶⁴, then the reaction must be Zn⁶⁴(He³, γ)Ge⁶⁷, where the Ge⁶⁷ then undergoes β⁺ decay to Ga⁶⁷. If this were the reaction mechanism, the γ rays from the decay of Ge⁶⁷ should be detected, since the half-life of Ge⁶⁷ is 19 min.³² This was not the case.

Another more likely possibility exists. The small amount of Zn⁶⁶ impurity (~0.14%) is sufficient to give the reaction Zn⁶⁶(He³, np)Ga⁶⁷. If the cross section is calculated using the stated amount of Zn⁶⁶, the resulting excitation function is plotted in Fig. 6. This excitation function is indeed large when compared with similar reactions for He³ on Zn⁶⁴ (see Fig. 3). Since no other explanation seems feasible, this is assumed to be the reaction which takes place.

Other reactions involving He³ on Zn⁶⁶ are not likely to take place often enough to produce a sufficient quantity of any radioactive isotope to be detected. The (He³, α_p) reaction on Zn⁶⁶ to produce Cu⁶⁴ would require a cross section of several barns to compete with the (He³, 3p) reactions on Zn⁶⁴. The highly probable reaction Zn⁶⁶(He³, 2p) leads to the stable nucleus Zn⁶⁷, which cannot be detected.

CONCLUSIONS

This study has shown that the direct reactions induced by He^3 particles incident on a Zn^{64} target dominate compound-nuclear formation in the same entrance channel. One consequence is that the production of proton-rich isotopes by (He^3, xn) reactions for $x > 1$ is *not* favored over similar $[\alpha, (x+1)n]$ reactions, despite the more favorable Q values. This technique of cross-section extraction by means of radionuclide detection has proven to be a valuable and economic tool in reaction-mechanism studies.

ACKNOWLEDGMENTS

The authors wish to thank the staff and crew of the Cyclotron Laboratory at the University of Colorado for their aid and cooperation in making the bombardments. Special acknowledgments are due Don Zurstatt of the Cyclotron Laboratory for the considerable time he spent performing tasks with the computer. John Jarmer of the Physics Department at the University of Wyoming spent many hours helping calibrate the equipment and determining experimental unknowns.

†Work supported in part by the U. S. Atomic Energy Commission.

*Now at Barron Co. Campus, Stout State University, Rice Lake, Wisconsin.

‡Now at PPB, Inc., Research Reactor Facility, University of Missouri, Columbia, Missouri.

¹E. A. Bryant, D. R. F. Cochran, and J. D. Knight, *Phys. Rev.* **130**, 1512 (1963).

²D. D. Armstrong and A. G. Blair, *Phys. Rev.* **140**, B1226 (1965).

³R. H. Siemssen, T. H. Braid, D. Dehnhard, and B. Zeidman, *Phys. Letters* **18**, 155 (1965).

⁴G. B. Saha and N. T. Porile, *Phys. Rev.* **151**, 907 (1966).

⁵D. J. Baugh, G. J. B. Pyle, P. M. Rolph, and S. M. Scarrott, *Nucl. Phys.* **A95**, 115 (1967).

⁶R. J. Griffiths, *Nucl. Phys.* **A102**, 329 (1967).

⁷R. Balcarcel and J. A. R. Griffith, *Phys. Letters* **26B**, 213 (1968).

⁸N. W. Golchert, J. Sedlet, and D. G. Gardner, *Nucl. Phys.* **A152**, 419 (1970).

⁹G. B. Saha and N. T. Porile, *Phys. Rev.* **149**, 880 (1966).

¹⁰D. Bodansky, R. K. Cole, W. G. Cross, C. R. Gruhn, and I. Halpern, *Phys. Rev.* **126**, 1082 (1962).

¹¹P. H. Stelson and F. K. McGowan, *Phys. Rev.* **133**, B911 (1964).

¹²N. T. Porile, *Phys. Rev.* **115**, 939 (1959).

¹³M. Cogneau and L. J. Gilly, *Nucl. Phys.* **73**, 122 (1965).

¹⁴J. P. Hazan and M. Blann, *Phys. Rev.* **137**, B1202 (1965).

¹⁵N. T. Porile, I. Fujiwara, and R. L. Hahn, *Phys. Rev.* **170**, 958 (1968).

¹⁶I. Fujiwara and N. T. Porile, *Phys. Rev.* **173**, 1055 (1968).

¹⁷R. L. Hahn, *Anal. Chem.* **40**, 219 (1968).

¹⁸C. M. Fou, R. W. Zurmühle, and J. M. Joyce, *Nucl. Phys.* **A97**, 458 (1967).

¹⁹M. G. Betigeri, H. H. Duham, R. Santo, R. Strock, and R. Bock, *Nucl. Phys.* **A100**, 416 (1967).

²⁰Y. W. Yu and M. Blann, *Phys. Rev.* **170**, 1131 (1968).

²¹Foils loaned to the University of Wyoming by the Physics Division, Los Alamos Scientific Laboratory, Los Alamos, New Mexico.

²²D. A. Lind, J. J. Kraushaar, R. Smythe, and M. E. Rickey, *Nucl. Instr. Methods* **18**, 62 (1962).

²³Energy loss for He^3 particles in zinc was calculated from data given for He^3 ranges in copper [M. Rich and R. Madey, University of California Radiation Laboratory Report No. UCRL-2301, 1954 (unpublished), p. 364].

²⁴A. H. Jaffey, *Nucleonics* **18**, No. 11, 180 (1960).

²⁵Y. Beers, *Introduction to the Theory of Error* (Addison-Wesley, Reading, Mass., 1957).

²⁶G. D. Chase and J. L. Rabinowitz, *Principles of Radioisotope Methodology* (Burgess Publishing Company, Minneapolis, Minn., 1969), 3rd ed.

²⁷T. R. King, J. J. Kraushaar, R. A. Ristinen, R. Smythe, and D. A. Stupin, *Nucl. Instr. Methods* **88**, 17 (1970).

²⁸T. K. Oh, Ph.D. thesis, University of Colorado, 1970 (unpublished).

²⁹University of Colorado Cyclotron Laboratory Progress Reports, 1968–1970 (unpublished).

³⁰C. Détraz, private communication.

³¹C. Détraz, C. E. Moss, C. D. Zafiratos, and C. S. Zaidins, *Phys. Rev. Letters* **26**, 448 (1971).

³²*Nucl. Data* **B2**, No. 6, 73 (1968).